sciendo

*Polish Journal of Chemical Technology, 26, 1, 39—50, 10.2478/pjct-2024-0005*

# Characteristics and applications of iron oxides reduction processes

**K.S. Abdel Halim[1, 2*], A.A. El-Geassy[2], M.I. Nasr[2], Mohamed Ramadan[1, 2], Naglaa Fathy[3], Abdulaziz S. Al-ghamdi[1]**

[1]College of Engineering, University of Ha'il P.O. 2440 Hail, Saudi Arabia; mrnais3@yahoo.com; a.alghamdi@uoh.edu.sa0.000

[2]Central Metallurgical Research and Development Institute (CMRDI), P.O. Box 87, Helwan 11421, Egypt; elgeassy@hotmail.com; minasr@hotmail.com

[3]Department of Physics, College of Science, University of Hail, P.O. Box 2440, Hail, Saudi Arabia; n.ismail@uoh.edu.sa

[*]*Corresponding author: e-mail:* k.abdulhalem@uoh.edu.sa

The present review handles the main characteristics of iron oxide reduction and its industrial applications. The reduction of iron oxide is the basis of all ironmaking processes, whether in a blast furnace or by direct reduction and/or direct smelting processes. The reduction characteristics of iron ores control the efficiency of any ironmaking process and the quality of the produced iron as well. Many controlling parameters should be considered when discussing the reducibility of iron ores such as equilibrium phase diagrams, reduction temperature, pressure, gas composition, and the nature of both iron ores and reducing agent. The different factors affecting the main routes of ironmaking will be highlighted in the present review to give a clear picture for each technology. Moreover, further innovations regarding the reduction of iron oxides such as reduction by green hydrogen will be discussed.

**Keywords:** ironmaking; iron oxides; reduction; extractive metallurgy; green hydrogen.

## INTRODUCTION

Iron is considered one of the most common elements in the earth's crust, representing about 5% by weight among elements of the earth's crust, and the fourth abundant element after oxygen, silicon, and aluminium. Iron is an allotropic element that has three different forms at atmospheric pressure depending upon temperature; (α-Fe, BCC) body centred cubic stable below 910 °C, (γ-Fe, FCC) face centred cubic exists between 910 °C and 1390 °C, and the last phase is (δ-Fe, BCC) body centred cubic which is stable at 1390 °C to 1539 °C [1]. Iron has three solid oxides, namely hematite ($Fe_2O_3$), magnetite ($Fe_3O_4$), and wüstite ($Fe_xO$: x is a little lower than unity). The specific volumes of these ox-ides are 0.272, 0.270, and 0.231 ml/g iron, respectively[2]. Maghemite ($\gamma$-$Fe_2O_3$) is also a common phase for iron III oxide. It has the same chemical formula as hematite. It is a ferrimagnetic material and considered the ultimate low-temperature oxidation product of magnetite ($Fe_3O_4$) and inverts to rhombohedral hematite ($\alpha$-$Fe_2O_3$) when heated at temperatures between 250 and 750 °C. In nature, it is usually found only around the edges of regions of hydrothermal or magnetic activity, where the temperature ranges from 300 to 400 °C. Table 1 shows the different forms of iron ore minerals, and their specifications. Iron exists naturally in minerals (iron ores) in the form of iron oxides such as hematite (69.9% Fe), magnetite (72.3% Fe), carbonate such as siderite (~ 48.2% Fe), and limonite (brown ores), $Fe_2O_3$ $xH_2O$.

Industrially, the only known way to extract iron from its ores is the reduction technique, whether in a blast furnace or by direct reduction and/or smelting. The driving force that determines the reduction of iron oxides is the removal of oxygen from the ore. The reduction characteristics of iron oxides and their equilibrium with the reductant determine to a great extent the efficiency of any ironmaking process. The phase diagrams of iron with oxygen, hydrogen and/or carbon systems should be considered when discussing the reducibility of iron oxides. However, ironmakers classify the reduction techniques of iron oxides according to the type of reducing agent into gaseous reduction (by $H_2$, CO, or mixture of them), and carbothermic reduction by solid carbon. Both reduction techniques are mainly depending on many factors such as reduction temperature, pressure, gas composition, and nature of the reactants.

In general, the reduction temperature is the main factor affecting the rate of reduction of iron oxides. The reduction rate of iron oxides is found to be increased by increasing reduction temperature[3–14]. Experimentally, it was found that, at a given temperature, the rate of reduction (dr/dt) is highest at the beginning of the reduction process followed by a gradual decrease in the rate till the end of the processes. The reduction of iron oxide is a complex process that takes place in more than one step (stepwise manner) via the formation of intermediate lower oxide phases such as magnetite and/or wűstite depending on the applied reduction temperature. Some literature[15–19] observed the presence of reduction rate minimum temperature phenomena at later stages, in which the reduction rate has a minimum degree at certain temperature, after which the rate increases again with further rise in reduction temperature. Such rate minimum phenomena that were observed during the gaseous reduction of iron oxide was explained in terms of physical and/or chemical changes. The formation of some hard reducible phases such as fayalite and ferrites, sintering effects as well as α-γ Fe phase transformation (912 °C) are the most factors affecting rate minimum phenomena[20]. It has been reported that the diffusion velocity of $H_2O$ or $CO_2$ in γ-Fe is much slower than that

**Table 1.** Types and specifications of iron ore minerals

| Ore mineral | Chemical formula | % Fe | Sp. gravity |
|---|---|---|---|
| Oxides: | | | |
| Hematite | $Fe_2O_3$ | 70 | 5–6 |
| Magnetite | $Fe_3O_4$ | 72.4 | 5.5–6.5 |
| Goethite | $Fe_2O_3.H_2O$ | 62.9 | 4.0–4.4 |
| Limonite | $Fe_2O_3.nH_2O$ | 48-63 | 3.6–4.0 |
| Carbonates: | | | |
| Siderites | $FeCO_3$ | 49.3 | 3.7–3.9 |
| Sulfides: | | | |
| Pyrrhotite | FeS | 61.5 | 4.6 |
| Pyrite | $FeS_2$ | 46.7 | 4.9–5.2 |

in α-Fe resulting in a lower rate of reduction at > 912 °C than that at lower temperature[1].

The reduction temperature has a great influence on the structure of the produced iron and its lattice strain[21–22]. By decreasing the reduction temperature, the pore structure becomes finer. The lattice strains can be induced in iron powders reduced in hydrogen or carbon monoxide at low temperatures, whereas reduction at higher temperature allows relief of these strains by atom movement.

The reducing gas composition and its partial pressure play a great role in the stability of the reduced metallic iron. It was found that the rate of formation of metallic iron is increased with increasing partial pressure of the reducing gas. A highly porous structure with extensive surface cracking could be observed under strongly reducing gas composition[23–27].

The main characteristics of iron ores (nature, type, and amount of impurities) greatly affect the reduction of iron oxide. The surface orientations, dislocations, impurities in solid solution and the non-stoichiometry of solid phase change to a great extent the rate of reduction of iron oxides[28–32]. In general, iron ores naturally occur with impurities such as silica and oxides of Ca, Al, Mg, Mn and others. These impurities decrease the reduction rate of iron oxides in all ironmaking processes and affect the reduction kinetics as well[33–40]. Accordingly, it is important to investigate the iron ore composition and the impurities levels when considering any ironmaking process.

On the other hand, the reduction technique of iron oxides in micro and/or nanoscale might be extended to other novel and advanced applications. The reduction of iron oxides with green hydrogen is considered as the key parameter for decreasing greenhouse gas (GHG) in iron and steel industry to minimize the emission of $CO_2$. In this case, the green hydrogen is used as a reductant and fuel as well. The generated green hydrogen from the electrolysis of water can be utilized in ironmaking processes to replace carbonous materials with the target of minimizing $CO_2$ emission. Furthermore, the reduction of iron oxides is becoming a promising route for the fabrication of iron-metal alloys. Such technology is mainly dependent on the simultaneous reduction and sintering of iron oxide enforced metal oxides. Recently, this route became an important technique in powder technology. It can be used in developing intermetallic alloys with unique properties and looked upon as novel technology for the production of alloys such as Fe-Mo, Fe-Cr, Fe-Ni, and other nano-structured Fe-M intermetallics.

Based on the above background, the present review handled the commercial technologies applied for iron oxide reduction. The factors affecting the reduction of iron oxides in most ironmaking techniques are investigated in detail together with the theoretical bases of each technique.

## REDUCTION KINETICS AND MECHANISMS

The reduction of iron oxide takes place in more than one step via the formation of lower oxides ($Fe_2O_3 \rightarrow Fe_3O_4 \rightarrow FeO \rightarrow Fe$). These steps are greatly dependent on the applied temperature in both isothermal or non-isothermal techniques. In non-isothermal conditions, the reduction of iron oxide was carried out with reducing gas mixtures ($H_2$ and/or CO) from room temperature up to a pre-determined temperature. Different heating rates were also controlled (° C/min) and the extent of reduction was continuously measured from the $O_2$-weight loss resulting from the reduction reactions [$O_2$ + $H_2$ (CO) = $H_2O$ ($CO_2$)]. The typical reduction reactions of $Fe_2O_3$ with Ar-4 % $H_2$ gas mixture were performed in TG-DTA Thermal Analyzer (STA 409 NETZSCH, Germany) as given in Figure 1. The course of reduction was carried out at a heating rate of 5 °C/min up to 900 °C and kept constant at this temperature for 60 min. then cooled down to room temperature at a heating of 20 °C/min. From Figure 1, it can be detected the presence of one exothermic peak at about 530 °C and two endothermic peaks at 710 and 830 °C. The exothermic peak resulted from $Fe_2O_3$-$Fe_3O_4$ phase transformation, while the endothermic peaks were corresponding to $Fe_3O_4$-$Fe_xO$ and $Fe_xO$-Fe phase transformations, respectively. These phases were identified by applying X-ray phase analysis which confirmed the above-mentioned findings.

On the other hand, the isothermal reduction behaviour of iron oxide was carried out at certain temperatures. In these experiments, the sample was heated up to the pre-determined temperature in Ar atmosphere and kept constant for a while, then the reducing gas ($H_2$) was introduced instead of Ar and the reduction was followed by measuring the $O_2$-weight loss as a function of time and continued till completion where no more weight loss could be recorded. Figure 2 represents the typical reduction behaviour of iron oxide in $H_2$ atmosphere at 700–1000 °C. It shows that the rate of reduction increased with rise in the reduction temperature. At a given temperature, the rate of reduction is high at the early stages and then gradually decreases with progress in the reduction reactions showing a significant delay in the reduction rate at the later stages. The delay in the rate is more pronounced at lower temperatures, which is attributed to wüstite–iron transformation step[41].

It was reported in most ironmaking literature that the rate-controlling step of the reduction of iron oxide is the oxygen removal from wüstite phase ($Fe_xO \rightarrow Fe$ transformation step). The reduction reaction mechanism can be predicted from the correlation between the following:

1 – Apparent activation energy ($E_a$ kJ/mole) calculated from applying Arrhenius equation;

$$K_r = K_o . e^{-Ea/RT} \quad (1)$$

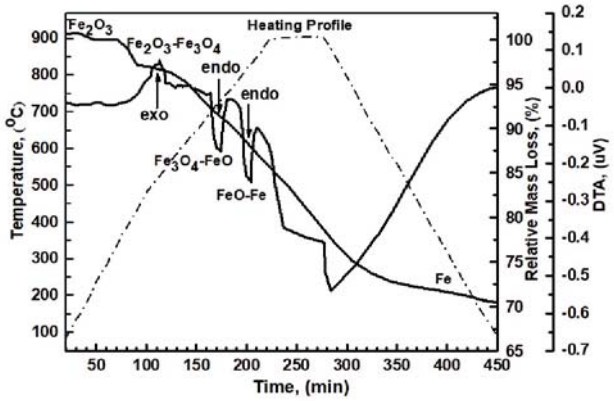


**Figure 1.** TG-DTA thermal analysis for iron oxide non-isothermally reduced in 4% $H_2$-Ar gas mixture in pure 5 °C/min $H_2$ up to 900 °C

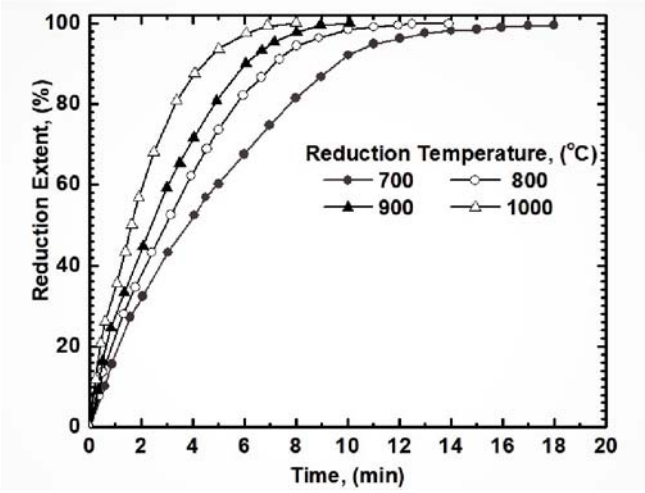


**Figure 2.** Typical isothermal reduction behavior of iron oxide reduced at 700–1000 °C in pure 0.5 l/min $H_2$ atmosphere

where; $K_r$ is the rate constant, $K_o$ is the frequency factor, R is the gas constant, and $T$ is the absolute temperature.

2 – Microscopic examination of morphology and structure of partially and completely reduced samples using both Reflected Light Microscope (RLM) and Scanning Electron Microscope (SEM-attached with EDAX). This will give a good idea about the mode of reaction, especially in the case of dense grains.

3 – Testing of different mathematical formulations derived from the gas–solid reaction model (interfacial chemical reaction, chemical reaction and mixed control reaction equations) to predict the mechanism of reaction from the straight line obtained[42].

It has been reported that in the gas-solid reactions of iron oxides, the following basic processes were proposed[1, 43–45]:

i) Diffusion of the reducing gases from the bulk gas to the surface of grains or the diffusion of the product gases in the reverse directions through the boundary layer around the particles.

ii) Internal diffusion of these gases and possibly of cations and anions through the layer of solid particles to the reaction interface.

iii) Chemical reactions between the reducing gas and oxygen atoms either at a particular reaction interface or throughout the particles.

iv) Nucleation and grain growth of metallic iron on the surface of lower oxide.

v) Heat transfer to the reaction interface.

It has been agreed that the most important stage in the reduction reactions, which determines the reaction rate and the degree of utilization of gases, is the separation of $O_2$ from wűstite.

There are three possible mechanisms suggested for the gaseous reduction of dense iron ores depending upon the structure of the ore, all of them are based on the microstructure changes accompanying the reduction process as follows.

The first mechanism suggested by Edstrom[1] is the most widely accepted and applies to hard dense ore which produces a porous iron product layer on the surface of the ore particles. Oxygen is removed from the FeO/Fe interface only according to the reaction shown in equation (2). The other oxides are reduced as written in equations (3) and (4). For these two reactions, ferrous ions diffuse inward from the iron-wustite interface, where the oxygen is removed to react with magnetite and hematite.

At the FeO/Fe interface, the oxygen is up taken:

$$FeO + H_2\ (CO) = H_2O\ (CO_2) + Fe \quad (2)$$

While other oxides can be reduced:

$$Fe_3O_4 + Fe^{2+} + 2e = 4\ FeO \quad (3)$$

$$4Fe_2O_3 + Fe^{2+} + 2e = 3\ Fe_3O_4 \quad (4)$$

The second mechanism was proposed in literature[44] in which the reducing gas ($H_2$) takes the oxygen from the oxides at the iron oxides interfaces:

$$FeO + H_2 = Fe + H_2O \text{ (at the FeO/Fe interface)} \quad (5)$$

$$Fe_3O_4 + H_2 = 3FeO + H_2O \text{ (at the } Fe_3O_4 \text{ /FeO interface)} \quad (6)$$

$$3Fe_2O_3 + H_2 = 2Fe_3O_4 + H_2O \text{ (at the } Fe_2O_3/Fe_3O_4 \text{ interface)} \quad (7)$$

The third mechanism proposed in the literature45 can apply to coarsely crystallized ores. A dense iron is formed around grains of wüstite. Both hematite and magnetite are reduced into lower oxides, but in this interpretation, wüstite is reduced by $H_2$ (or CO) to metallic iron which is then absorbed on the outer surface. Oxygen ions diffuse through the iron band to the surface and react with $H_2$ to form $H_2O$ vapour.

The predicted reduction mechanisms from applying a mathematical model can be confirmed through investigating the morphology and microstructure changes accompanying the reduction process. Figures 3 and 4 show different images for the morphology of reduced metallic iron. In all experiments, the iron oxide is reduced partially and/ or completely in $H_2$ atmosphere at 1000 °C. The microstructure of partially reduced iron oxide at early and intermediate stages is given in Figure 3 (a), in which different phases of lower oxides are clearly distinguished. Whereas the morphology of completely reduced iron oxide can be observed in Figure 3 (b), a relatively porous structure of metallic iron with micro and macro pores can be detected. Figure 4 (a) shows the SEM image of completely reduced iron oxide, in which a porous iron layer can be simply observed. The sintering phenomena accompanying the reduction process at high temperatures is shown in Figure 4 (b) – a very dense metallic layer of iron with the absence of macropores is observed.

## INDUSTRIAL TECHNOLOGIES FOR IRONMAKING

The extraction of iron from its ores via the reduction technique is the main step in all ironmaking technologies. To date, ironmaking processes take 3 general routes; namely blast furnace (BF), direct reduction (DR), and direct-smelting route (DS). All technologies used in the three routes have their own advantages and disadvantages. However, it is difficult to carry out a direct comparison between them, as BF technology is well established and represents an essential route for manufacturing iron from iron ores. The different factors affecting the three routes will be highlighted hereinafter to give a clear picture of each technology, but still, the most difficult question to be answered is the suitable route that can be recommended for new ironmaking investment. The main deriving forces that should be considered when

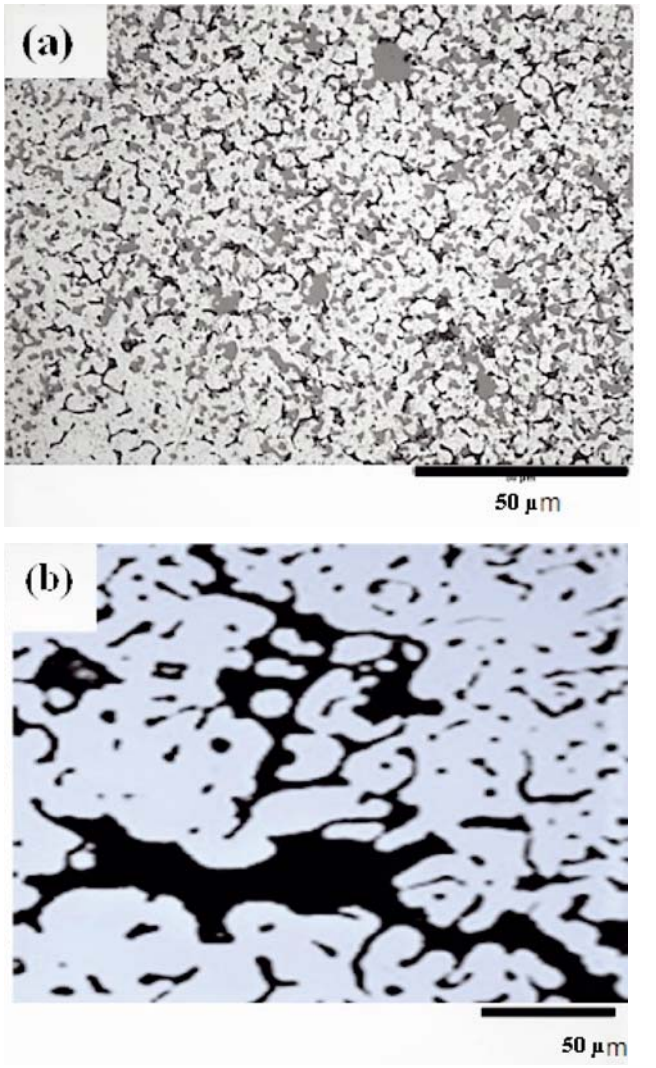


**Figure 3.** Morphology of iron oxide reduced at 1000 °C by $H_2$ under different operation conditions: (a) partially reduced to 50%, (b) completely reduced to metallic iron

answering such kind of questions are (not limited to) the available energy resources, iron ores, capital and fixed production costs, and environmental regulations.

**Blast Furnace**

Iron blast furnace is still the essential route for production of molten iron to date. The ironmaking blast furnace (BF) is a very energy-intensive metallurgical process and the prime route for steel production, from which about 70% of the world's steel consumption is produced. It depends on using low or medium iron ores together with coke to produce hot metal after the separation of gangue materials as slag. Apart from the complicated thermodynamics phenomena occurring in blast furnace, the highly capital-intensive cost is the most important factor when selecting BF technology to produce hot metal. This is because BF requires coke ovens to convert raw coal to coke, sinter plant for preparing iron ores, gas cleaning, and control systems. However, the current modern blast furnace with amazing characteristics of the operation indices as shown in Table 2 will continue to be the main route for the production of hot metal[46–50]. The innovation in the design together with the improvement in the operation parameters are the main reasons to keep the blast furnace route a competitive technology to date.

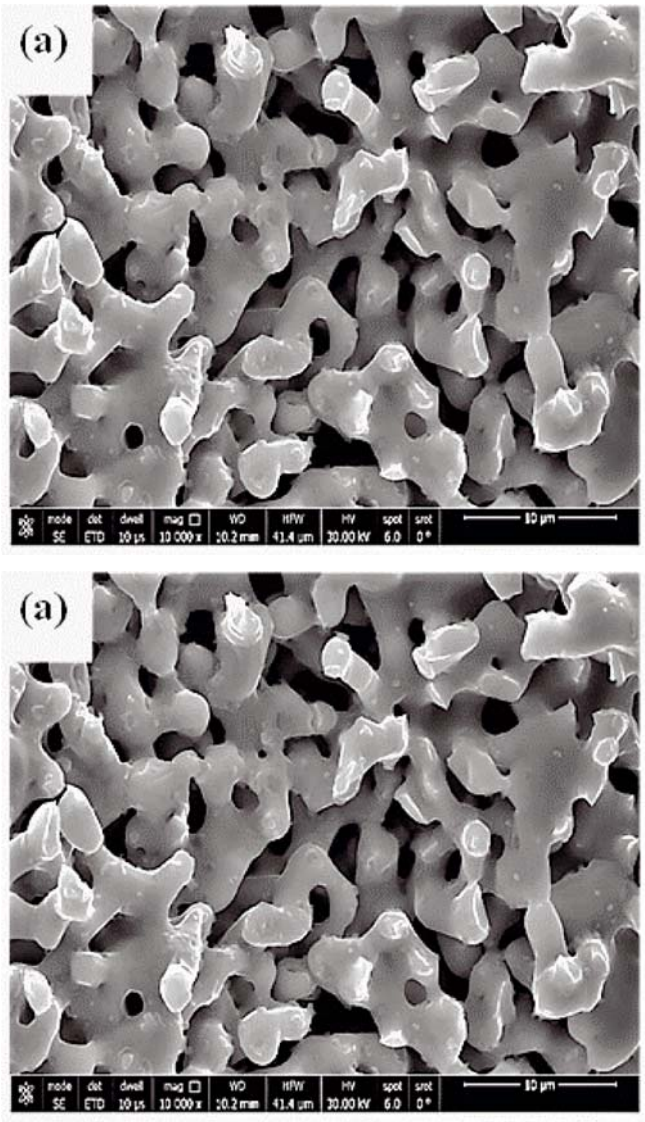


**Figure 4.** Photomicrographs of iron oxide reduced at 1000 °C by $H_2$ gas: (a) completely reduced $Fe_2O_3$, (b) reduced $Fe_2O_3$ after sintering for 5 hr

Innovations in measuring tools and the use of advanced mathematical models have radically enhanced the ways of controlling and monitoring the blast furnace operation parameters. Still, lowering energy consumption with keeping higher productivity are the main goals of blast furnace makers that can be achievable via increasing oxygen enrichment air blast and extensive coal injection, and/or looking for new source of energy. Artificial Intelligent programmes are nowadays trying to develop more advanced ways to solve the complicated blast furnace operation problems.

However, to define the importance of reduction processes in modern blast furnace technology, it is essential to understand the relation between iron ore composition and fuel consumption. As mentioned previously, the reducibility of iron oxide and the associated impurities in the iron ores include many complicated reactions because the reduction of these oxides takes place in more than one reaction (stepwise manner). The presence of different intermediate lower oxides and metal ferrites hindered the reduction reaction in a general way. In blast furnace processes, the reduction of iron oxide takes place by solid carbon of coke and/or mixture of CO and $H_2$ coming from natural gas (NG) injection

**Table 2.** Modern blast furnace characteristics

| | |
|---|---|
| Types of fuel | Coke, Pulverized coal, Natural gas |
| Maximum hearth diameter, m | 15.6 |
| Maximum production rate, ton per day | 12,000 - 13,500 |
| Average fuel rate, kg/ton hot metal | 450 (coke) or 275 kg coke + 175 kg coal |
| Blast furnace efficiency, % | 88–95 |
| Si content in hot metal, % | 0.2 |
| Average campaign life, year | 15 |

(90–99% $CH_4$). Accordingly, the blast furnace reactions could be classified into two categories, namely indirect reduction (reaction 8), and direct reduction (reaction 9). Thermodynamically, each reaction has its own characteristics in terms of heat consumption and the amount of reducing agent[51];

$$FeO + \left(\frac{1}{\mathrm{k1}} + 1\right) CO = Fe + CO_2 + \left(\frac{1}{k_1}\right) CO \qquad \Delta H_{T1} = -13.1 \frac{kJ}{mol}.Fe \tag{8}$$

$$FeO + C = Fe + CO \qquad \Delta H_{T2} = 15.4 \frac{kJ}{mol}.Fe \tag{9}$$

(where $k_1$ = equilibrium constant, ΔH = enthalpy of the reaction).

It was reported that one of the most important factors that lead to a decrease in the amount of coke consumption is the decrease in the percentage of direct reduction reactions. This can be done in modern blast furnaces by increasing the amount of natural gas injected through tuyeres or via injection pulverized coal. Many blast furnace operators use the degree of direct reduction as an important index to optimize the blast parameters of iron blast furnace. Thus, the amount of natural gas injected via tuyeres could be increased to the maximum value that corresponds to the minimum percentage of direct reduction of iron oxide.

In related investigations of the authors of the present review[47, 52–53], and other literature[54], different mathematical models were developed to optimize the operation parameters of blast furnace technology. These models mainly depend on the calculations of direct reduction reaction, which can be used to measure and control the operation parameters of blast furnace. The detail of each model is discussed hereafter.

### Mathematical model of theoretical coke consumption

One of the important indexes that define the efficiency of iron blast furnace is the amount of coke consumption. The coke is the main source of energy in the blast furnace. It is recommended to operate BF with a minimum amount of coke. Andronov in literature[54] developed PDK model to estimate the minimum theoretical value of coke consumption based on Equations 8 and 9. In that model, the minimum degree of direct reduction ($r_{dmin}$) corresponding to the minimum amount of coke consumption is calculated from Equation (10).

$$r_{d_{\min}} = \frac{\frac{1}{\bar{\eta}_{CO}} - n\left[2\frac{\bar{\eta}_{H_2}}{\bar{\eta}_{CO}} - \frac{Q_{CH_4}}{Q_{C_t}} + 1\right] - \bar{\eta}_{CO} C_i^h}{\frac{1}{\bar{\eta}_{CO}} + \frac{\Delta H_1}{Q_{C_t}} + 1} \tag{10}$$

where $\bar{\eta}_{CO}$ is the degree of utilization of CO in the reaction (FeO + CO = Fe + $CO_2$). The equilibrium constant of the reaction is $k_1$,

$$\left(\log k_1 = \frac{949}{T} - 1.134, \quad k_1 = 0.47 \text{ at } 1173K, \ \bar{\eta}_{CO} = 0.32\right)$$

($\bar{\eta}_{H_2}$ is the degree of utilization of $H_2$ in the reaction (FeO + $H_2$ = Fe + $H_2O$) the equilibrium constant of the reaction is $k_2$

$$\left(\log k_2 = -\frac{977}{T} + 0.64; \quad k_2 = 0.64 \text{ at } 1173K, \ \bar{\eta}_{H_2} = 0.39\right)$$

$n$ = mole of $CH_4$, $\Delta H_1$ = enthalpy of direct reduction of iron oxide, J/mol (Fe)

$\bar{Q}_{C_t}$ = heat given by coke carbon burning at the tuyeres in the heat exchange zone of the furnace (T = 1173 K), J/mol ($C_t$)

$\bar{Q}_{CH_4}$ = heat given by 1 mole of methane in the heat exchange zone of the furnace, J/mol($CH_4$).

The theoretical minimum coke consumption ($K_{min}$) and minimum carbon in coke ($C_{min}$) could be estimated using the value of $r_{dmin}$ as the following:

$$C_{\min} = \frac{1 - r_{d_{\min}}}{\bar{\eta}_{CO}} - 2n\frac{\bar{\eta}_{H_2}}{\bar{\eta}_{CO}} - n \ , \qquad K_{\min} = \frac{C_m + C_e}{C_k} \tag{11}$$

(where $C_k$ = carbon content in coke, and $C_e$ = carbon content in hot metal).

It was reported that the injection of natural gas enriched with oxygen into BF increases the chance of lowering the direct reduction percentage to minimum value and consequently decreases the total coke consumption with conditions keeping other parameters in acceptable indices. The model could be used in BF technique to predict the effect of different factors on the relative coke consumption.

### Mathematical model of theoretical flame temperature and energy balance

The energy balance in iron blast furnace is a very complicated issue due to the high temperature in the raceway region which makes the actual measurement difficult. However, the operators of iron blast furnace use the theoretical flame temperature (TFT) as an operational index for blast furnace parameters optimization. The actual temperature in the raceway is lower than the theoretical flame temperature because all heat losses are ignored in the calculation. Accordingly, increasing the calculation accuracy of TFT enables optimizing the operation parameters of iron blast furnace. Furthermore, TFT can be used as a controlling parameter to detect any deviations from the normal operation of the furnace.

The mathematical model of TFT estimation depends on the concentration of the raceway gases namely CO, $H_2$, and $N_2$ together with the amount of coke carbon. In the combustion zone, the burning of coke carbon reaching the tuyeres and methane can be estimated for 1 mole of air blast using the following stoichiometric equation:

$$(2\omega+\varphi-D)C_t+\omega O_2+(1-\omega)N_2+\varphi H_2O+DCH_4=$$
$$=(2\omega+\varphi)CO+(1-\omega)N_2+(\varphi+2D)H_2 \quad (12)$$

where; $\omega$, $\varphi$, and $D$ are oxygen, moisture and natural gas contents in dry blast, respectively.

The contents of raceway gases ($m^3/m^3$) can be calculated from Equation (13).

$$V_{CO}=\frac{2\omega+\varphi}{1+\omega+2\varphi+2D} \quad V_{N_2}=\frac{1-\omega}{1+\omega+2\varphi+2D}$$
$$V_{H_2}=\frac{\varphi+2D}{1+\omega+2\varphi+2D} \quad (13)$$

Using the enthalpy of hot blast ($i_b^{'}$), enthalpy of carbon of coke burning to slag temperature ($i_C$) and enthalpy of auxiliary fuel, the total enthalpy of raceway gases ($i_\Phi$) can be estimated from Equation (14).

$$i_\Phi=\frac{\frac{12}{22.4}\left[(2\omega+\varphi)(W_C+i_C)-Di_C\right]+i_b^{'}}{1+\omega+2\varphi+2D} \quad (14)$$

where; $W_C$ is the heat of combustion of coke carbon in CO (kJ/kg coke carbon).

The TFT can be estimated from Equation (15).

$$t_T=\frac{i_\Phi}{C_0} \quad (15)$$

**Mathematical model of air blast calculation**

Abdel Halim in literature[47], developed a mathematical model to estimate the volume of air blast consumption based on the bases of the above-mentioned models. The model is mainly based on the value of direct reduction of iron together with estimation of hydrogen consumption during indirect reduction of iron by hydrogen ($V_{H2i}$). Thus, the most accurate index that can be used in the calculation of ($r_d$) is the ratio of degree of utilization of $H_2$ and CO inside the furnace ($R=\frac{\eta_{H_2}}{\eta_{CO}}$). The value of R is varied in a very narrow range (0.95–1.0). The selected value of R could be confirmed by zone heat balance for iron blast furnace. The air blast consumption can be calculated using nitrogen balance in Equation (16).

$$\upsilon_{N_2}^{'}(C_\phi+C_{NG}V_{NG})=V_{T.G.}N_2 \quad (16)$$

where $\upsilon'_{N2}$ is the nitrogen consumption of air blast per kg coke carbon reaching the tuyeres ($C_\Phi$).

$$\upsilon_{N_2}^{'}=\frac{0.9333N_{2_b}}{1+0.5\varphi-N_{2_b}},\ \ m^3/kgC_\phi \quad (17)$$

$$N_{2_b}=\frac{V_{T.G}N_2(1+0.5\varphi)}{0.9333(C_\phi+C_{NG}V_{NG})+V_{NG}N_2} \quad (18)$$

Since $V_b=V_{T.G.}\frac{N_2}{N_{2b}}$ (19)

$$V_b=\frac{0.9333(C_\phi+C_{NG}V_{NG})+V_{T.G.}N_2}{1+0.5\varphi},\ \ m^3/tHM \quad (20)$$

In conclusion, all the above mathematical models have been demonstrated to investigate the effect of different operation parameters on the performance and efficiency of blast furnace, and consequently the total cost of hot metal production. Figure 5 shows the analysis of real data for blast furnaces using mathematical models developed in the above models[47, 52]. It can be reported that the increasing amount of injected natural gas via

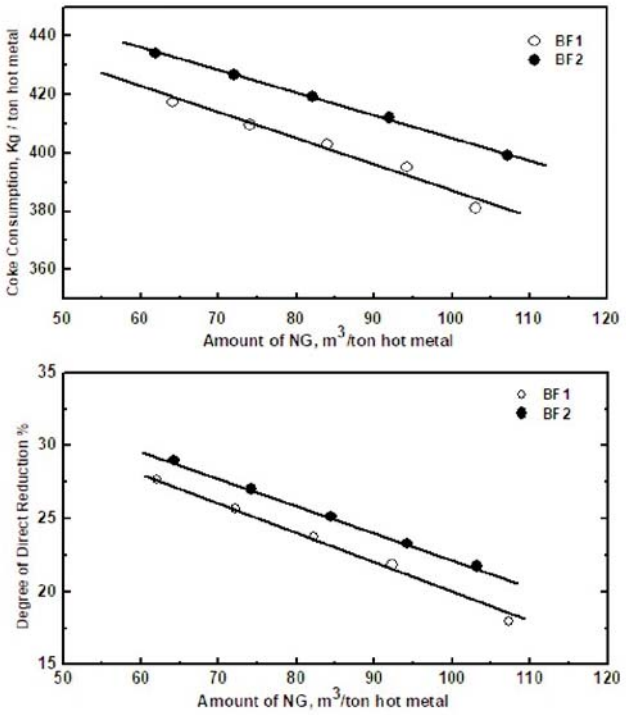


**Figure 5.** Analysis of real data for iron blast furnace using mathematical models

tuyeres greatly affects the value of sharing degree of direct reduction and consequently decreases the coke consumption and consequently, the total cost of the production will be declined. The most important benefit of using mathematical models in iron blast furnace is to predict any deviation from normal conditions and enable the blast furnace operators to take the right decision in a reasonable time.

**Direct Reduction Technologies**

Direct reduction (DR) technique is an alternative route for the production of DRI or so-called sponge iron from its ores instead of conventional blast furnace. It was invented to eliminate the use of coke and replace it with non-coking coal or natural gas in the reduction reactions. In DR processes, iron ore in the form of fines, lumps, and/or pellets is reduced by either solid or gaseous reducing agents at relatively lower temperatures (below the melting and fusion temperatures of ores or agglomerates). In DR processes, iron ore is reduced in solid state form at 800–1050 °C by either reformed natural gas (>95% $CH_4$) or coal-based reductant. By time, the number of BFs in the world is decreasing with increasing the number of DR plants. The main product of DR processes is DRI (Direct Reduced Iron) or sponge iron, which is the main charge of electric steel furnaces (as scrap). The recent development of beneficiation methods, as well as pelletizing of iron ores, enables the DR techniques to be promising and very competitive to iron blast furnace route. In reality, the invention of DR technique in 1930 was a target for further beneficiating of iron ore to increase blast furnace performance[55]. The DR processes is intrinsically more energy efficient than the BF since they operate at low temperatures and the produced DRI (90–94% metallization) which is successfully used as a feed for electric furnaces in mini steel plants for steel production. Hot briquetting technology

is also applied to produce Hot Briquetting Iron (HBI) from the fines produced during the charging of furnace and/or from the movement of pellets or lumps during the reduction process. This technique is applied to prevent the reduced metallic iron from the re-oxidation reactions before shipping, handling and storage of DRI. However, the first successful plant to produce DRI was developed by Midrex Technologies, Inc in the late 1950s. Before the end of 1960's, most electric arc furnaces used DRI as the main feed.

Ironmakers classify the DR techniques according to the type of reductant (coal based DR and gas-based DR processes) and furnace used into different DR processes[56, 57]. Table 3 summarizes the characteristics of the common types of direct reduction processes. High grade of iron ore is reduced at relatively low temperatures using the product of reformed natural gas ($H_2$ + CO) or coal. The DR technique became a suitable route to produce iron in many developing countries suffering from lack of coking coal. The main DR technologies of gas-based DR processes that produces >85% of DRI are Midrex and HyL.

**Table 3.** Common types of DR/HBI processes

| Process/Index | Midrex | HYL/Energiron | PERED (Persian DR) | Rotary Kiln |
|---|---|---|---|---|
| Type of furnace | shaft | Retort | shaft | Rotary |
| Productivity, in 2020, Mt | 62.63 | 12.95 | 3.0 | 25.47 |
| Type of reductant | gaseous | gaseous | gaseous | coal |

Midrex technology is the most common route of DR in terms of production and popularity. According to the annual report of statistics of Midrex (2020 world direct reduction) as shown in Table 4, the total world production of DRI was 104.4 million tons (Mt) in 2020[57]. It decreased by 3.4% from the record 108.1 Mt produced in 2019. From 2015–2019, worldwide DRI output increased by 35.5 Mt, or nearly 49%. India is ranked number one among all countries in the rate of DR production by 32.98 million tons in 2020.

**Table 4.** Statistical analysis for world DRI in 2020

| | |
|---|---|
| The total world production of DRI, Mt | 104.4 |
| Total production of DRI by Midrex technology, Mt | 62.63 |
| The total production of DRI for the top 5 nations, Mt (Top 5 nations ranked in DRI production: India, Iran, Russia, Saudi Arabia, Mexico) | 81.48 |
| Total production of DRI by shaft furnaces in, Mt | 78.67 |
| Total production of DRI by Middle East and North Africa countries in, Mt | 50.04 |

The prevailing chemical reaction in DR processes is the heterogeneous gas-solid reduction of $Fe_2O_3$ with $H_2$ + CO (coming from natural gas reforming) as the following[56, 58–63], $Fe_2O_3$ ($O_2$ content = 30 %) to $Fe_3O_4$ ($O_2$ content= 27.7 %), to FeO ($O_2$ content = 22.3%), and then the final product is Fe:

*Hematite reduction to magnetite:*

$$3Fe_2O_3 + CO = 2Fe_3O_4 + CO_2 \quad \Delta H = +52.85\ kJ/mol \tag{21}$$

$$3Fe_2O_3 + H_2 = 2Fe_3O_4 + H_2O \quad \Delta H = -11.59\ kJ/mol \tag{22}$$

$$Fe_3O_4 + CO = 3FeO + CO_2 \quad \Delta H = +36.46\ kJ/mol \tag{23}$$

$$Fe_3O_4 + H_2 = 3FeO + H_2O \quad \Delta H = +77.59\ kJ/mol \tag{24}$$

*Wüstite reduction to metallic iron:*

$$FeO + CO = Fe + CO_2 \quad \Delta H = -17.13\ kJ/mol \tag{25}$$

$$FeO + H_2 = Fe + H_2O \quad \Delta H = +24.00\ kJ/mol \tag{26}$$

In Midrex technology[56], the reduction of iron ores takes place in a vertical shaft furnace using the product of reformed natural gas. The process contains three main units namely, shaft furnace, the reforming unit of NG, and the cooling system. The efficiency of the process is greatly affected by the reduction temperature, composition of the reducing gas, and the nature of the feedstock charge. However, a major problem facing the steel industry all over the world, including the developing countries, has been the inadequate availability of high-quality scrap. This has been accentuated by the ever-increasing adoption of continuous casting. While the technology for making quality steels requires large quantities of prime quality scrap, continuous casting improves energy utilization and reduces the generation of in-plant scrap. In conclusion, DRI becomes a promising substitution for scrap due to very low contamination, particularly the contents of sulfur and phosphorus in the metallic iron.

On the other hand, HyL III processes was developed to reduce iron oxide in the form of lump and/or pellets in two stages in retorts. The reduction reactions were performed with natural gas-steam reforming to produce (1:3 $CO/H_2$ gas mixture). However, a single moving bed reactor is developed to replace the four-bed reactor in HyL I and can be operated by 100% iron ore pellets, 100% lump ore, or a mixture of both (70% pellets + 30% lump ore). The Steam-natural gas mixture is preheated to 620 °C in a reformer convection section before entering the reformer at 830 °C to produce reducing gas.

$$C_nH_{(2n+2)} + n\ H_2O \rightarrow nCO + (2n\text{-}1)\ H_2 \tag{27}$$

The chemical composition of the reducing gas is; 73% $H_2$, 17% CO, 6% $CO_2$, 1% $H_2O$ and 3% $CH_4$. The HyL IV is a shaft furnace in which the natural gas is reformed in the same reactor by the freshly reduced metallic iron (DRI) which acts as a catalyst for the reforming of natural gas. At the same time in the reactor, water – shift gas reaction is simultaneously proceeded ($CO + H_2O = CO_2 + H_2$).

**Direct-Smelting Process (DS)**

The direct smelting (DS) technique is considered the second alternative ironmaking technology. The DS processes are characterized by using non-coking coal, and in some cases possible fine ores instead of pellets or lump ores. The absence of restrictions in most DS processes for both types of iron ores and/or reducing agents makes the DS processes very competitive although most of the invented techniques are still on the research scale or pilot plant. So, the advantage of this technique is the lower capital cost results from the elimination of the coke and agglomeration plants and high smelting intensities. The most common commercial DS proces-

ses are Corex, Finex, Technored, and HIsmelt[50, 64–75]. Recently, the Corex and Finex processes have reached industrial application. The main disadvantage of DS processes is the lower production rate. The module capacity of Corex process in a commercial scale is about 0.6 Mt/y, although a new Corex module was constructed at Baosteel in Chain with average capacity 1.5 Mt/y. The most important challenge facing DS processes is the high capital cost because the process does not use coal directly. However, Corex process involves two main reactors. The first unit is the pre-reduction furnace that reduces iron ore to 90%. The second unit is the melter-gasifier that finally reduces and smelts the iron ore and generates reducing gas by combustion of coal for the pre-reduction furnace. In all DS processes, there are many chemical reactions associated with different mass and energy transport phenomena. One novel idea is now being used to decrease the cost efficiency of the Corex process through recycling the top gases that can be utilized in power generation or can be exported to the neighbour direct reduction plant[70].

## FURTHER INNOVATIONS

### Reduction of iron oxide with green hydrogen

The iron and steel industry is an energy-intensive sector as it requires huge natural resources. To date, the main reducing agent used in the reduction of iron ores in all ironmaking processes is based on carbonous sources such as coke, coal, pulverized coal, and even natural gas. About 7% of the global greenhouse gas is produced from iron and steel industry. One of the novel technologies suggested to minimize $CO_2$ emission during reduction of iron oxides is to replace carbonous materials with green hydrogen. For example, replacing coke of blast furnaces with green hydrogen which is produced from water electrolysis has the potential to reduce emissions of $CO_2$[76–79]. The hydrogen produced from electrolysis of water is now becoming a core principle of new process configurations for decarbonized many heavy industries. A mathematical model based on mass and energy balance has been developed[76] to explore the feasibility of using hydrogen direct reduction of iron ore (HDRI) coupled with electric arc furnace (EAF) for carbon-free steel production. The results show that such technology could reduce the emissions from steel production in the EU by more than 35%.

The electrolysis of water that produces $H_2$ and $O_2$ involves many exchange transport phenomena. The energy required for the electrolysis processes may be obtained from emerging renewable power sources such as wind and/or solar[77] which makes the process more feasible in the near future. However, the total decarbonization degree will depend on the amount of green hydrogen that can replace carbon in the reduction processes. In real ironmaking processes, the complete reduction of iron oxide by hydrogen is feasible from the theoretical point of view, but in reality, other factors should be considered such as the reduction of iron ore impurities, and hard reducible phases. In general, the carbon of coke used in blast furnace for example is not only used as a source of reductants, but also it is the main source of energy.

Hydrogen-based direct reduction is among the most attractive solutions for green ironmaking, with high technology readiness. In general, hydrogen-based direct reduction proceeds two to three times faster than CO--based direct reduction. This is attributed to the physical properties of hydrogen, i.e., its small molecule size, low viscosity, and high mobility when diffusing as a molecule through pores or as dissociated atom through solids. The hydrogen-based direct reduction process is characterized by a hierarchy of phenomena that can influence the reaction at different length and time scales. They range from transport and reaction kinetics in a shaft reactor at macroscopic scale down to chemical reactions at interfaces at atomic scale and catalysis, dissociation, and charge transfer at electronic scale. Reaction kinetics is also affected by micro-to-atomic-scale features of the different oxides and the adjacent iron layers, including crystal defects, porosity, mechanics, and local composition. Although these dynamically evolving nano-/microstructure features can alter the kinetics by orders of magnitude, a complete picture of their roles and interactions is still missing. More research is still needed to take the final decision for completely replacing carbon by green hydrogen in ironmaking processes.

### Manufacturing of metallic alloys

The reduction technique of iron oxide has been extended to be applied in other metallurgical applications. The reduction of iron oxide powder is a promising route for the fabrication of iron-metal alloys. Such technique might replace the traditional route for manufacturing these alloys by powder metallurgy in the near future. It is mainly dependent on simultaneous reduction-sintering reactions of iron oxide-doped metal oxides. The reduction technique is a simple, environmentally friendly, and economical approach to developing intermetallic alloys with unique properties.

The authors of the present work have successfully produced metallic materials with a wide range of applications via the reduction route[80–86]. The composition of the produced alloys can be controlled under operational conditions. The first example is the synthesis of ferronickel (Fe-Ni alloy) with different contents of Ni via gaseous reduction of blended oxides ($Fe_2O_3$+NiO) by hydrogen gas. The reduction of metal oxides takes place as given in the following reactions:

$$2Fe_2O_3 + 3H_2 = 4Fe + 3H_2O \quad (28)$$

$$NiO + H_2 = Fe + H_2O \quad (29)$$

$$Fe_2O_3 + NiO = NiFe_2O_4 \quad (30)$$

$$NiFe_2O_4 + 4H_2 = Ni + 2Fe + 4H_2O \quad (31)$$

The reduction temperature and the composition of the starting materials play an important role in the reduction kinetics and mechanisms. It was reported that NiO is more easily reducible than $Fe_2O_3$, and hence the formation of metallic nickel during the reduction of blended oxide accelerates the reduction rate of iron oxide because Ni acts as a catalyst[80–82]. However, the idea of using a gaseous reduction technique to fabricate Fe-M alloys might be applied to Fe-Co, Fe-Mn, Fe-Mo, W-Fe, W-Fe-Ni.

Another example of utilizing the reduction technique in powder technology was used to fabricate heavy tungsten alloy with composition 93W:3Ni:2Fe:2Co[84–85]. It was reported that the oxide blend composed of $WO_3$, NiO, $Fe_2O_3$, and $CoO_3$ can be reduced under certain conditions in hydrogen atmosphere at temperature above 900 °CC to avoid the appearance of residual oxides. The reduction rate increased with increasing reduction temperature. A very dense intermetallic matrix was formed after sintering at 1500 °C as shown in Figure 6[84]. Arrhenius plots and gas solid reactions equations were used to elucidate the reaction mechanism. It was found that the reduction rate is most likely controlled by the interfacial chemical reaction mechanism.

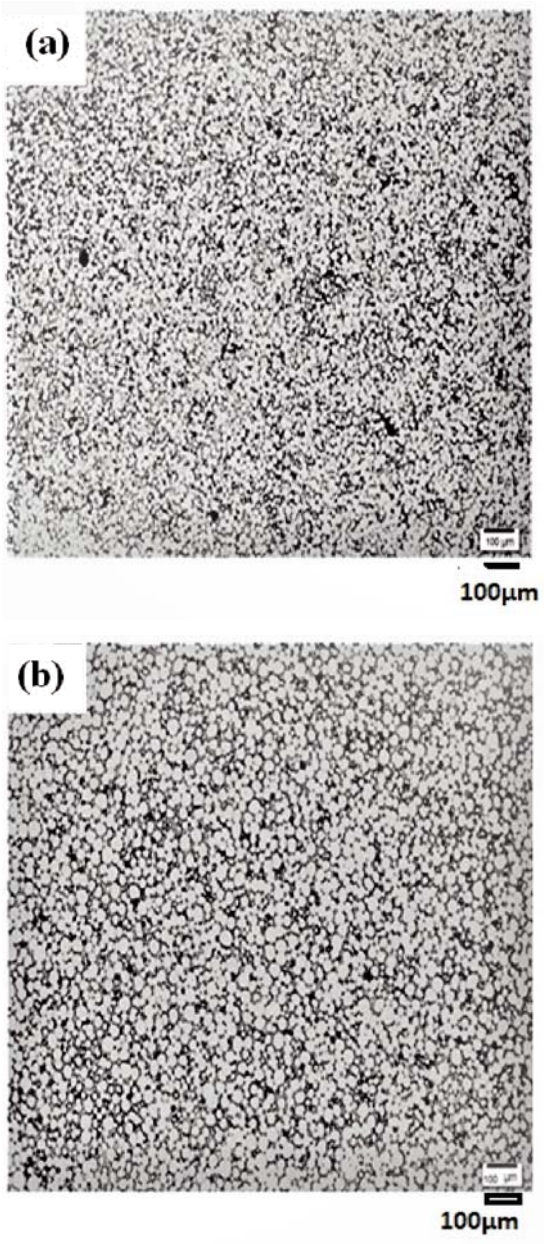


**Figure 6.** Photomicrographs of heavy tungsten alloy sintered at 1500 °C for:(a) 30 min, (b) 90 min

**Reduction of iron oxide in nanoscale**

Recently, nano-sized iron oxide has become an attractive material and promising candidate in different engineering applications[83, 87–89]. The reduction of nano--sized iron oxides is considered an important step in many metallurgical processes[87–93]. Experimental analysis showed that the reducibility of nano-sized iron oxide is much easier than micro-sized iron oxide. In all cases, this can be attributed to the high surface area of nano-sized iron oxide which facilitates the penetration of gas and consequently enhances the overall reduction process. It was reported that nano-sized iron oxide is reduced at relatively lower reduction temperature than commercial one. In related investigations[88], authors of the present work handled the reducibility of iron oxide nanoparticles with an average crystallite size of 35, 100 and 150 nm synthesized by hydro-thermal techniques. The nanoparticles were reduced isothermally in pure hydrogen at 400–600 °C. The influence of crystal size and reduction temperature on the reduction characteristics of nano-sized iron oxide was deeply investigated together with predic-

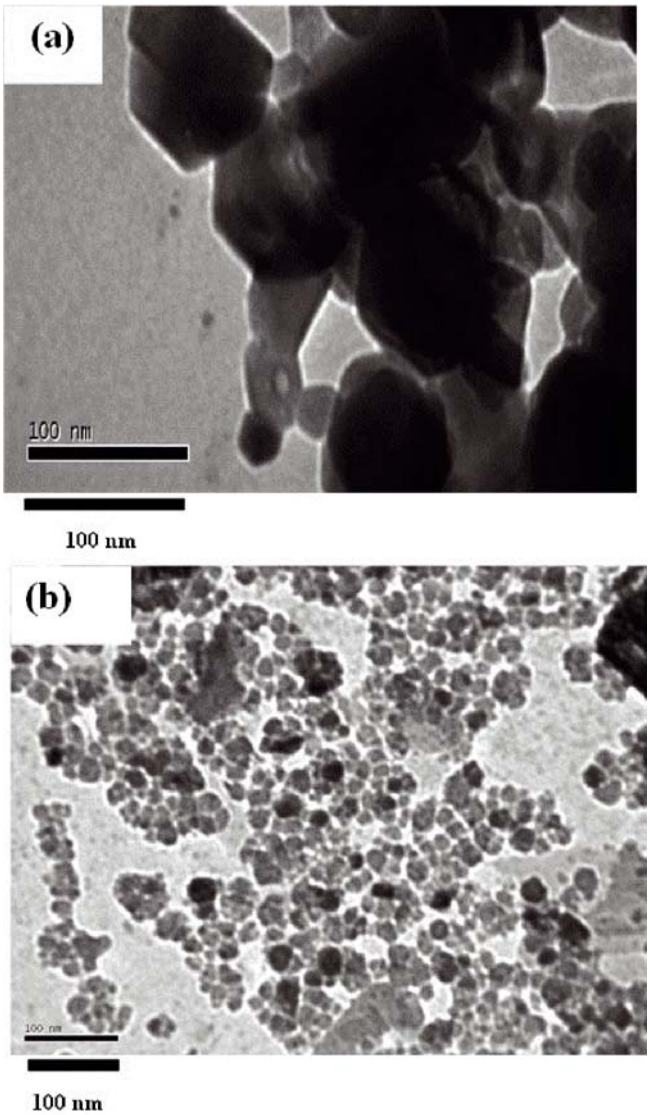


**Figure 7.** TEM images of iron oxide nanoparticles (35 nm): (a) unreduced, (b) reduced particles with $H_2$ gas at 450 °C

tion of reduction mechanisms in nanoscale. The TEM images of both reduced and unreduced nanoparticles (35 nm) are shown in Figure 7. The reduction behaviour of nanoparticles in pure hydrogen gas at different reduction temperatures is recorded in Figure 8. It was observed that the complete reduction of nanoparticles was detected at a reduction temperature ≥ 450 °C. A topochemical mode of reduction was observed with

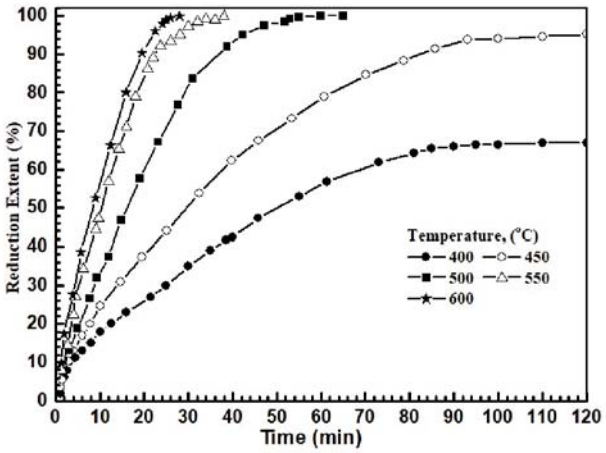


**Figure 8.** Reduction behaviour of iron oxide nanoparticles (35 nm) reduced at different reduction temperatures

all reduced samples. The reduction process was initially controlled by the combined effect of gas diffusion and interfacial chemical reaction mechanism whereas the controlled mechanism at the final stages of reduction was varied according to the size of nanoparticles.

Although the investigation of reduction technique for nano-sized iron oxide is still in the research stage, it can be recommended to test the utilization of nano-sized iron oxide in ironmaking processes as a new source for decreasing energy consumption. The nano-sized iron oxide powder can be injected with air blast in iron blast furnace like the current pulverized coal injection technology. Such kind of injection will decrease the reduction time of iron ore charge and consequently, the energy consumption will decline[83].

## CONCLUSIONS

The reduction technique of iron oxide is a significant issue in many engineering applications. It is considered the main operation in all ironmaking processes, whether blast furnace, direct reduction and/or direct smelting. The reduction of iron ores is the only way to extract iron from its ores by gaseous or carbothermic techniques. The reduction characteristics and factors affecting the reduction kinetics and mechanisms play an important role in optimizing all ironmaking processes on an industrial scale. The present review highlighted the advanced trends in ironmaking processes with special emphasis on the reduction techniques of iron oxide. Although there has been a great effort to develop and optimize the main three technologies of ironmaking (BF, DR, and DS) in the last decades, more innovations are still needed to overcome the current problems in each technology. The reduction of iron oxides by green hydrogen and utilizing nano-sized iron oxides are among novel trends to optimize ironmaking processes. Besides that, the reduction of iron oxide doped metal oxides can be utilized to produce Fe-M intermetallics alloys with unique properties. However, any new trend in the reduction of iron oxides should be investigated in detail to become competitive and easy to apply commercially. Developing energy-efficient technologies based on nanotechnology and nanomaterials of iron oxides, together with encouraging research to further improve the beneficiation of iron ores, are becoming hot issues in the ironmaking field.

## ACKNOWLEDGEMENTS

This research has been funded by the Scientific Research Deanship at University of Ha'il – Saudi Arabia through project number RG-22 028.

## LITERATURE CITED

1. Edström, J.O. (1953). The mechanism of reduction of iron oxides. *J. Iron Steel Inst*. 175, 289–304.

2. Moon, J.T. & Walker, K.D. (1975). Swelling of iron oxide compacts during reduction. *Ironmaking & Steelmaking*, 1, 30–35.

3. Spreitzer, D. & Schenk, J. (2019). Reduction of Iron Oxides with Hydrogen—A Review. Res. Internat. 20(10), 1900108. DOI: 10.1002/srin.201900108.

4. Srinivisan, N.S. & Lahiri, A.K. (1977). Studies on the reduction of hematite by carbon. Metal. Trans. B. 8, 175. DOI: 10.1007/BF02656367.

5. Bryk, C. & Lv, W.K. (1986). Continuous Reduction of iron ore with coal in an electrically heated furnace. The Canadian *J. Mater. Sci.* 25(3), 241–246. DOI: 10.1179/cmq.1986.25.3.241.

6. Haque, R., Ray, H.S. & Mukherjee, A. (1993). Reduction of iron ore fines by coal fines in a packed bed and fluidized bed apparatus — A comparative study. *Metall. Mater Trans B*. 24, 1993, 511–520. DOI: 10.1007/BF02666434.

7. Morrison, A.L., Wright, J.K. & Bouling, K. McG. (1978). Microstructure of metallized iron ore pellets reduced by coal char in a rotary kiln simulator. *Ironmaking & Steelmaking*, 5(1), 39–44.

8. El-Geassy, A.A. & Nasr, M.I. (1990). Effect of sintering on the structure of hematite and its behaviour during reduction. Canadian Metallurgical Quarterly, 29(3), 185–191. DOI: 10.1179/cmq.1990.29.3.185.

9. Davis, C.G., McFarlin, J.F. & Pratt, H.R. Direct-reduction technology and economics. (1982*). Ironmaking & Steelmaking,* 9(3), 93–129.

10. Unal, A. & Bradshow, A.V. (1983). Rate processes and structural changes in gaseous reduction of hematite particles to magnetite. Metall. Trans. 14, 743–752.

11. Abdel Halim, K.S.Nasr, M.I. & El-Geassy, A.A. (2011). Developed model for reduction mechanism of iron ore pellets under load. *Ironmaking & Steelmaking*, 38, 189–196. DOI: 10 .1179/030192310X12816231892305.

12. El-Geassy, A.A., Nasr, M.I., El-Raghy, S.M. & Hammam, A.E. (2020). Comparative studies on isothermal and non-isothermal reduction of hematite in carbon monoxide atmosphere. *Ironmaking & Steelmaking*, 47, 948–957. DOI: 10.1080/03019233.2019.1646564.

13. Bahgat, M., Abdel Halim, K.S. , El-Kelesh, H.A. & Nasr, M.I. (2011).Behaviour of wüstite prepared from Baharia iron ore sinter during reduction with $CO–CO_2–N_2$ gas mixture. Mineral Processing and Extractive Metallurgy (Trans. Inst. Min. Metal. C). 120(2), 102. DOI: 10.1179/1743285510Y.0000000010.

14. El-Geassy, A.A. & Rajaumar, V. (1985) Influence of particle size on the gaseous reduction of wüstite at 900–1100 °C. Trans. ISIJ, 25, 1022.

15. Shehata, K.A. & Ezz, S.Y. (1973). Study of the last stages or reduction of iron oxides. Trans. IMM, 82 C, 638.

16. El-Geassy, A.A., Nasr, M.I. & Omar, A.A. (1990). The fourteen congress IMM, 2-6 July (pp 29). London, UK.

17. El-Geassy, A.A. (1986). Gaseous reduction of $Fe_2O_3$ compacts at 600–1050 ° C. *J. Mat. Sci*. 21, 3889–3900. DOI: 10.1007/BF02431626.

18. Nasr, M.I. (1985). Structural analysis in gas solid reaction. Ph. D. Thesis, Cairo University, Egypt.

19. Hessien, M., Kashiwaya, Y., K. Ishii, K., Nasr, M.I. & El-Geassy, A.A. (2008). Characterization of iron ore

sinter and its behaviour during non-isothermal reduction conditions. *Ironmaking & Steelmaking,* 35(3), 183–190. DOI: 10.1179/174328107X174663.

20. El-Geassy, A.A., Shehata, K.A. & Ezz, S.Y. (1977). Mechanism of iron oxide reduction with hydrogen/carbon monoxide mixtures. *J. Iron-Steel Inst*. 17(11), 629–635. DOI: 10.2355/isijinternational1966.17.629.

21. Turkdogan, E.T. & Vinters, J.V. (1974). Catalytic effect of iron on decomposition of carbon monoxide: I. carbon deposition in $H_2$-CO Mixtures. Metal Trans B. 5, 11–19. DOI: 10.1007/BF02642919.

22. Okura, A. & Metsuahita, Y. (1965). On the properties of reduced sponge-iron powders. Testu-To-Hagane, 51, 11. DOI: 10.2355/tetsutohagane1955.51.1_11.

23. Towhidi, N. & Szekely, J. (1980). An experimental study of hematite reduction with $CO+H_2$ mixtures over the temperature range 600–1300 ° C. *J. Metals*. 32(12), 420.

24. Wang, H. & Sohn, H.Y. (2012). Effects of Reducing Gas on Swelling and Iron Whisker Formation during the Reduction of Iron Oxide Compact. *Steel Res. Int*. 83(9999), 1-7. DOI: 10.1002/srin.201200054.

25. P. Cavaliere, P., Perrone, A. & Marsano, D. (2023). Effect of reducing atmosphere on the direct reduction of iron oxides pellets. *Powder Technol*. 426 (118650). DOI: 10.1016/j.powtec.2023.118650.

26. Mckewan, W.K. (1962). Trans. TMS-AIME. 224, 2, 387–393.

27. Sato, K.. Ueda, Y., Nishikawa, Y. & Goto, T. (1986). Effect of Pressure on Reduction Rate of Iron Ore with High Pressure Fluidized Bed. *J. Iron-Steel Inst*. 26(8), 697. DOI: 10.2355/isijinternational1966.26.697.

28. Turkdogan, E.T. & Vinters, J.V. (1971). Gaseous reduction of iron oxides. 1. Reduction of hematite in hydrogen. Met. Trans. 2(11), 3175–3188.

29. Turkdogan, E.T. & Vinters, J.V. (1972). Gaseous reduction of iron oxides: Part III. Reduction-oxidation of porous and dense iron oxides and iron. Met. Trans. 3, 1561–1574. DOI: 10.1007/BF02643047.

30. El-Geassy, A.A. & Nasr, M.I. (1990). Influence of the original structure on the kinetics and mechanisms of carbon monoxide reduction of hematite compacts. *J. Iron-Steel Inst.* 30(6), 417–425. DOI: 10.2355/isijinternational.30.417.

31. Abdel Halim, K.S., Bahgat, M., El-Kelesh, H.A. & Nasr, M.I. (2009). Metallic Iron Whisker Formation and Growth during Iron Oxide Reduction: Basicity Effect. *Ironmaking & Steelmaking,* 36(8), 631. DOI: 10.1179/174328109X463020.

32. Bahgat, M., Abdel Halim, K.S., Nasr, M.I. & El-Geassy, A.A. (2008). Morphological Changes Accompanying the Gaseous Re-duction of SiO2- Doped Wüstite Compacts. *Ironmaking & Steelmaking,* 35(3), 205–212. DOI: 10.1179/174328107X155259.

33. Abdel Halim, K.S. (2007). Isothermal reduction behavior of $Fe_2O_3$/MnO composite materials with solid carbon. *Mater. Sci. Eng.* A, 452–453, 15–22. DOI: 10.1016/j.msea.2006.12.126.

34. Bahgat, M., Abdel Halim, K.S. , Nasr M.I. & El-Geassy A.A. (2007). Reduction Behavior of Wüstite Doped with MgO. *Steel Res. Int.* 78(6), 443–450. DOI: 10.1002/srin.200706228.

35. Bahgat, M., Abdel Halim, K.S. , El-Kelesh H.A. & Nasr, M.I. (2011). Behaviour of wustite prepared from Baharia iron ore sinter during reduction with $CO–CO_2–N_2$ gas mixture. Mineral Processing and Extractive Metallurgy (Trans. Inst. Min. Metal. C). 120(2), 102. DOI: 10.1179/1743285510Y.0000000010.

36. El-Geassy, A.A. (1996). Gaseous reduction of pure $Fe_2O_3$ and MgO-doped $Fe_2O_3$ compacts with carbon monoxide at 1173–1473 K. *J. Iron-Steel Inst*. 36, 1328–1337.

37. El-Geassy, A.A. (1997). Stepwise reduction of CaO and/or MgO doped-$Fe_2O_3$ compacts to magnetite then subsequently to iron at 1173–1473K. *J. Iron-Steel Inst*. 37, 844–853. DOI: 10.2355/isijinternational.37.844.

38. El-Geassy, A.A., Nasr, M.I., Omar, A.A. & Mousa, E.A. (2007). Reduction kinetics and catastrophic swelling of MnO2-doped Fe2O- compacts with CO at 1073–1373K. *J. Iron-Steel Inst*. 47(3), 377–385. DOI: 10.2355/isijinternational.47.377.

39. El-Geassy, A.A. (1999). Influence of Doping with CaO and/or MgO on Stepwise Reduction of Pure Hematite Compacts. *Ironmaking and Steelmaking* 26(1), 41–52. DOI: 10.1179/irs.1999.26.1.41.

40. El-Geassy, A.A. (1996). Reduction of CaO and/or MgO-doped Fe2O3 compacts with carbon monoxide at 1173–1473K. *J. Iron-Steel Inst*. 36(11), 1344–1353. DOI: 10.2355/isijinternational.36.1344.

41. Abdel Halim, K.S., El-Geassy, A.A. , Ramadan, M.; Nasr, M.I., Hussein, A., Fathy, N. & Alghamdi, A.S. (2022). Reduction Behavior and Characteristics of Metal Oxides in the Nanoscale. *Metals*, 12(12), 182. DOI:10.3390/met12122182.

42. Szekely, J., Evans, J. & Sohn, H.Y. (1976). Gas Solid Reactions. Academic Press. New York, USA. Retrieved by AlChE (1977). 23(4). DOI: 10.1002/aic.690230435.

43. Morrison, A.L., Wright, J.K. & Bouling, K.McG. (1978). Direct reduction of iron ore pellets in a rotary kiln simulator. *Ironmaking and Steelmaking,* 5(1), 32–38.

44. McKewan, W.K. (1965). Steel Making, the Chipman Conference.141. MIT Press, Cambridge. Ed. J.F. Elliott.

45. Lien, H.O, El-Mehairy A.E. & Ross, H.U. (1971). A two-zone theory of iron oxide reduction. *J. Iron-Steel Inst*. 209, 451–545.

46. Babich, A. & Senk, D. (2015). Recent developments in blast furnace iron-making technology, Elsevier, Mineralogy, Processing and Environmental Sustainability, Pages 505–547, DOI: 10.1016/B978-1-78242-156-6.00017-4.

47. Abdel Halim, K.S. (2013). Theoretical approach to change blast furnace regime with natural gas injection. *J. Iron Steel Res. Internat.* 20(9), 40–46. DOI: 10.1016/S1006-706X(13)60154-5.

48. Wang, Y., Zuo, H. & Zhao, J. (2019). Recent progress and development of ironmaking in China as of 2019: an overview. *Ironmaking & Steelmaking,* 2020, 47(5), 1–10. DOI: 10.1080/03019233.2020.1794471.

49. Chen, Y. & Zuo, H. (2021). Review of hydrogen-rich ironmaking technology in blast furnace. *Ironmaking & Steelmaking,* 48(6), 749–768. DOI: 10.1080/03019233.2021.1909992.

50. Aziz, I.H., Abdullah, M.M., Salleh, M.A., Ming, L.Y. et.al. (2022). Recent developments in steelmaking industry and potential alkali activated based steel waste: A Comprehensive review. Materials, 15, 1948. DOI: 10.3390/ma15051948.

51. Pavalov, M.A. (1949). Metallurgy of Pig Iron, Part II, Metallurgizdate, 628.

52. Abdel Halim, K.S., Andronov, V.N. & Nasr, M.I. (2009). Blast furnace operation with natural gas injection and minimum theoretical flame temperature. *Ironmaking and Steelmaking,* 36(1), 12–16. DOI: 10.1179/174328107X155240.

53. Abdel Halim, K.S. (2007). Effective utilization of using natural gas injection in the production of pig iron. Materials Letters, 61, 3281–3286. DOI:10.1016/j.matlet.2006.11.053.

54. Andronov, V.N. & Abdel Halim, K.S. (2001). Improvement of technology of blast furnace melting with combined blowing, *J. Ferrous Metals (Cherny Metall)*, 8, 25–30.

55. Kuang, S., Li, Z. & Yu. A. (2018). Review on modeling and simulation of blast furnace. Steel Research International 89 (1). DOI: 10.1002/srin.201700071.

56. Direct from Midrex, Third quarter. (2012).

57. Dutta, S.K. & Sah, R. (2016). Direct Reduced Iron: Production. Encyclopedia of Iron, Steel, and Their Alloys. CRC Press. DOI: 10.1081/E-EISA-120050996.

58. 2020 World direct Reduction Statistics by Midrex. (2021). World Steel Dynamics, WSD. New Jersy, U.S.A.

59. Schenk, J.L. (2006). FINEX®:From fine iron ore to hot metal. Proceedings of the innovations in ironmaking session of 2006. International symposium. Linz, Austria.

60. Sohn, H.Y. & Szekely, J. (1972). A structural model for gas-solid reactions with a moving boundary—III: A general dimensionless representation of the irreversible reaction between a porous solid and a reactant gas. *J. Chem. Eng. Sci*. 27 (4), 763–778.

61. Andronov, V.N. (2001). Modern Blast Furnace. Library of Saint Petersburg State Technical University, Russia.

62. Lu, W.L. (1999). Kinetics and mechanisms of direct reduced iron ore. In J. Feinman, & D. R. Mac Rae (Eds.), Direct reduced iron – Technology and economics of production and use. 43–57. Warrendale: The Iron & Steel Society.

63. Gudenau, H.W., Fang, J., Hirata, T. & Gebel, U. (1989). Steel Res. 60(314), 38.

64. Gransden, I.F. & Sheasby, J.S. (1974). The sticking of iron ore during reduction by hydrogen in a fluidized bed. Canadian Metallurgical Quarterly. 13(4), 649–657.

65. Schmole, P. & Lungen, H.B. (2012). From Ore to Steel-Ironmaking processes. Stahl und Eisen. 132(6), 29–38.

66. Lungen, H.B., Mulheims, K. & Steffen, R. (2001). State of the art of direct reduction and smelting reduction of iron ores. STAHL EISEN. 121(5), 35–47.

67. Kepplinger, W.L. (2009). Actual state of smelting-reduction processes in ironmaking. Stahl und Eisen.7, 43–45.

68. Bohm, C., Heckmann, H. & Grill, W. (2011). SVAI Smelting/Direct Reduction Technology, Proc. Metec In Steel Conf. Dusseldorf, 27 june-1 July 2011. Dusseldorf, Germany.

69. Schenk, J.L., Wallner, F. , Kepplinger, W.L., Shin, M.K., Cho, M. & Lee, I.O. (2000). Technology for an increased portion of fine ore in the COREX process. Scandin. *J. Metal*. 29(2), 81–91.

70. Anameric, B. & Kawatra, S.K. (2009). Direct iron smelting reduction processes.Mineral Processing & Extractive Metall. Rev. 30, 1–51. DOI: 10.1080/08827500802043490.

71. Boom, R. &Steffen, R. (2001). Recycling of scrap for high quality steel products. STEEL RES, 72(3), 91–96.

72. Fruehan, R.J., Astier, J.E. & Steffen, R. (2000). Status of direct reduction and smelting in the year of 2000. Proc. 4th European Coke and Ironmaking Congr. (ECIC 2000). 19–22 June, Paris, France.

73. Shim, Y. & Jung, S. (2018). Conditions for Minimizing Direct Reduction in Smelting Reduction Iron Making. ISIJ. 58(2). 274–281.

74. Chatterjee, A. (2005). A critical appraisal of the present status of smelting reduction-Part I From blast furnace to Corex. Steel Times International, 29(4), 23.

75. Burke, P.D. & Gul, S. (2002). December). HIsmelt—the alternative ironmaking technology. In Proceedings of International Conference on Smelting Reduction for Ironmaking, Jouhari, AK, Galgali, RK, Misra, VN, Eds (pp. 61–71).

76. Bhaskar, A., Assadi, M. & Nikpey Somehsaraei, H. (2020). Decarbonization of the Iron and Steel Industry with Direct Reduction of Iron Ore with Green Hydrogen. Energies. 13, 758. DOI: 10.3390/en13030758.

77. Ostadi, M., Paso, K.G., Rodriguez-Fabia, S., Qi, L.E., Manenti, F., Hillestad, M. (2020). Process Integration of Green Hydrogen: Decarbonization of Chemical Industries. Energies. 13(18), 4859. DOI: 10.3390/en13184859.

78. Wang, R.R., Zhao, Y.Q., Babich, A., Senk, D. & Fan, X.Y., (2021). Hydrogen direct reduction (H-DR) in steel industry—An overview of challenges and opportunities. *J. Clean. Prod.* 329, 129797. DOI: 10.1016/j.jclepro.2021.129797.

79. Ma, Y., Isnaldi R. Souza Filho, I.R.S., Bai, et.al. (2022). Hierarchical nature of hydrogen-based direct reduction of iron oxides. *Scripta Materialia*, 213, 114571. DOI: 10.1016/j.scriptamat.2022.114571.

80. Abdel Halim, K.S., Ramadan, M., Shawabkeh, A., Abufara, A. (2013). Synthesis and characterization of metallic materials for membrane technology. Beni-Suef University *J. Basic Appl. Sci*. 2, 72–79.

81. Abdel Halim, K.S. (2012). Novel synthesis of porous Fe–Ni ferroalloy powder for energy applications. *Materials Letter*, 68, 478. DOI: 10.1016/j.matlet.2011.11.048.

82. Abdel Halim, K.S., Khedr, M.H., Nasr, M.I. & Abdel Wahab, M. Sh., (2008). Carbothermic reduction kinetics of nanocrystallite $Fe_2O_3$/NiO composites for the production of Fe/Ni alloy. *J. Alloys Compounds*. 463, 585–590. DOI: 10.1016/j.jallcom.2008.02.026.

83. El-Geassy, A.A, Abdel Halim K.S. & Alghamdi A.S. (2023). A Novel Hydro-Thermal Synthesis of Nano-Structured Molybdenum-Iron Intermetallic Alloys at Relatively Low Temperatures. *Materials*, 16(7), 2736. DOI: 10.3390/ma16072736.

84. Abdel Halim, K.S., Bram, M., Buchkremer, H.P. & Bahgat, M. (2012). Synthesis of heavy tungsten alloy by thermal technique. *Ind. Engin. Chem. Res.* 51(50), 16354–16360. DOI: 10.1021/ie301947e.

85. Al-Kelesh, H., Abdel Halim, K.S., Nasr, M.I. (2016). Synthesis of heavy tungsten alloys via powder reduction technique. *J. Mat. Res*. 31(9), 2977–2986. DOI: 10.1557/jmr.2016.318.

86. Ahmed, H.M., El-Geassy A.A. & Seetheraman S. (2011). Kinetic studies of hydrogen reduction of NiO-$WO_3$ precursors in fluidized bed reactor. *ISIJ Int*. 51(9), 1359–1367. DOI: 10.2355/isijinternational.51.1383.

87. Abdel Halim, K.S., Ramadan, M., Shawabkeh, A. & Fathy, N. (2017). Developing nanomaterials for ironmaking processes: Theory and practice. *Appl. Mech. Mat*. 865, 3–8. DOI: 10.4028/www.scientific.net/AMM.865.3.

88. Abdel Halim, K.S., Khedr, M.H., Soliman, N.K. (2010). Reduction characteristics of iron oxide in nanoscale. *Mat. Sci. Technol*. 26(4), 445–452. DOI: 10.1179/026708309X1246 8927349253.

89. Khedr, M.H., Abdel Halim, K.S. & Soliman, N.K. (2009). Synthesis and photocatalytic activity of nano-sized iron oxides. *Mat. Letters*. 63, 598–601. DOI: 10.1016/j.matlet.2008.11.050.

90. Khedr, M.H., Abdel Halim, K.S., Soliman, N.K. (2008). Effect of temperature on the kinetics of acetylene decomposition over reduced iron oxide catalyst for the production of carbon nanotubes. *Appl. Surf. Sci.* 255, 2375–2381. DOI: 10.1016/j.apsusc.2008.07.096.

91. El-Sheikh, S.M., Harraz, F.A., Abdel-Halim, K.S. (2009). Catalytic performance of nanostructured iron oxides synthesized by thermal decomposition. *J. Alloys Comp*. 487, 716–723. DOI: 10.1016/j.jallcom.2009.08.053.

92. Lyadov, A.S, Kochubeev, A.A., Markova, E.B., Parenago, O.P., Khadzhiev S.N. (2016). Features of Reduction and Chemisorption Properties of Nanosized Iron (III) Oxide. *Petroleum Chem.* 56(12), 1134–1139.

93. Abdel Halim, K.S., Khedr, M.H., Nasr, M.I., El-Mansy A. (2007). Factors affecting catalytic oxidation of CO over nano-sized $Fe_2O_3$. *Mater. Res. Bull*. 42, 731–741. DOI: 10.1016/j.materresbull.2006.07.009.